Journal of Membrane Science 498 (2016) 374–384

Contents lists available at ScienceDirect

Journal of Membrane Science

journal homepage: www.elsevier.com/locate/memsci

A chlorine-tolerant nanofiltration membrane prepared by the mixed diamine monomers of PIP and BHTTM

Yong-Jian Tang, Zhen-Liang Xu *, Shuang-Mei Xue, Yong-Min Wei, Hu Yang

State Key Laboratory of Chemical Engineering, Membrane Science and Engineering R&D Lab, Chemical Engineering Research Center, East China University of Science and Technology, 130 Meilong Road, Shanghai 200237, China

ARTICLE INFO

Article history:
Received 9 May 2015
Received in revised form
7 October 2015
Accepted 10 October 2015
Available online 22 October 2015

Keywords:
Polysulfone UF membrane
Interfacial polymerization
Nanofiltration
Mixed diamine monomers
Chlorine-tolerant

ABSTRACT

Using Polysulfone (PSF) ultrafiltration (UF) membrane as porous support, a chlorine-tolerant nanofiltration (NF) membrane was prepared by interfacial polymerization of piperazine (PIP) and 2,2'-bis(1-hydroxyl-1-trifluoromethyl-2,2,2-triflutoethyl)-4,4'-methylenedianiline (BHTTM) mixture with trimesoyl chloride (TMC). The XPS, SEM, AFM and contact angle methods were employed to characterize the physicochemical properties and morphology of the prepared NF membranes. The effects of preparation conditions such as reaction time, monomers mixing ratio and oxidation treatment on NF membrane performance were investigated. The salt rejection of the NF membrane met the order of $Na_2SO_4 > MgSO_4 > NaCl$, indicating the membrane possessed a negative surface charge. The results showed the NF membrane prepared under the optimum conditions exhibited pure water flux (PWF) with 79.1 (L/m^2 h) and Na_2SO_4 rejection of 99.5% under 0.6 MPa. The optimized post oxidation condition was treated by 3000 ppm NaClO solution for 1 h. The best NF membrane had a molecular weight cut-off (MWCO) less than 300 Da, corresponding to the pore size of 1 nm, which was calculated from the rejection of carbohydrates. The robustness of the NF membrane was proven by showing satisfactory stability in the long time running.

1. Introduction

The demand for freshwater increases rapidly because of rapid population growth and industrial development. To deal with water scarcity, several methods have been developed to treat the waste water and reuse it. As a rising technology, membrane technologies have been demonstrated robust performances in reclamation, water treatment and desalination [1,2]. Nanofiltration (NF) is a membrane process between reverse osmosis (RO) and ultrafiltration (UF), which rejects solutes nominally 1 nm in dimension with MWCO ranging from 200 to 1000 Da [3–5]. With the advantage of high fluxes, low operating pressure, high rejection to divalent ions and low retention of monovalent ions, low investment and operation cost, the NF process has been widely applied in the softening of drinking water [6], the removal of heavy metals from wastewater [7–9], the concentration of the natural compound [10], and so on.

Nowadays, NF membrane material can be classified into two groups: aromatic polyamides (PA) and cellulose acetate (CA). The CA membrane has good resistance to chlorine while its drawbacks are obvious: narrow pH range, susceptible to microbial erosion, easy to creep under high pressure, thus leading to irreversible flux decline. On the other hand, PA membrane was stable over a wider pH range and had favorable transport property, which made PA a very popular NF material [11].

However, the free chlorine tolerance of the routine PA is not good. While free chlorine (such as: Cl_2, NaClO and so on) is widely used to disinfect or degrade the soluble organic matter during the pretreatment of the raw water. There always are some residual free chlorine in the pretreated water. When contacted with PA membrane, PA membrane will be irreversible degraded. To remove the residual free chlorine completely, will increase the running cost and the process complexity.

To improve the chlorine resistance of PA membrane, many methods have been developed. Such as: coating [12], grafting polymerization [13], developing new type of monomer [14], incorporating nanomaterial (CNT, GO) [15,16]. The fluorinated monomers are the arising materials [17]. The fluorine–containing groups (such as :–F, $–CF_3$) are the electron-withdrawing group, which can minimize N-chlorination and reduce the ring chlorination on the amine or the acid side. Murphy et al. [18] developed a series of PA membranes made of the acid chloride which had fluorine-containing groups (such as: monofluorotrimesoyl, nitrotrimesoyl chloride, perfluorotrimesoylchoride, perchlorotrimesoyl

* Corresponding author. Fax: +86 21 64252989.
E-mail address: chemxuzl@ecust.edu.cn (Z.-L. Xu).

http://dx.doi.org/10.1016/j.memsci.2015.10.028
0376-7388/

chloride) or the amine modified with the electron-withdrawing group(such as: 4-fluoro-m-phenylenediamine, 2-fluoro-m-diphenylenediamine, 3,5-diaminobenzotrifluoride, 4,6-difluorobenzene-1,5-diamine), and these PA membranes showed good resistance to chlorine.

In our previous work [19], a fluoropolyamide NF membrane with perfect chlorine-resistant property was formed through IP technique on the PES UF lab membrane with BHTTM and TMC employed as the monomers in aqueous and organic phases. After the oxidation treatment by NaClO, both the PWF and the salt rejection were improved greatly. However, if the PES UF lab membrane used in our previous work was instead by more hydrophobic basement membrane (such as PSF UF industrial membrane), the PWF of the NF membrane would not improve such greatly after NaClO oxidation treatment. The ideal NF membrane could not be obtained. Mixing different aqueous monomers is a feasible way to obtain the mixed polyamide NF membrane with high performance. Fang et al. [20] developed a mixed polyamide-based composite nanofiltration membrane.They found that because of the synergetic effect of PEI and PIP, both the water flux and the salt rejection improved. Shao et al. [21] fabricated a newly NF membrane by mixing the PIP/MPD, which showed a high rejection to dyes.

In this case, a mixed polyamide thin layer was synthesized by using PIP and BHTTM mixture in the aqueous phase and TMC in the organic phase through interfacial polymerization on the PSF UF membrane. The relationships between membrane property and the ratio of PIP and BHTTM were investigated thoroughly. Na_2SO_4, NaCl and $MgSO_4$ were used to characterize the rejections of polyamide/PSF flat sheet NF membranes. Glucose, sucrose, and raffinose were used to evaluate the MWCO and pore size of the NF membrane. The membrane structure and the physicochemical properties were analyzed by XPS, SEM, AFM and contact angle.

2. Experimental

2.1. Materials

Polysulfone (PSF) UF membrane (the MWCO and PWF are 50,000 Da and 125 L m^{-2} h^{-1} bar^{-1}, respectively.) supplied from the development center for water treatment technology (Hangzhou, China) was used as the support of the NF membrane. Trimesoyl chloride (TMC, $\geq$98%) was purchased from Qingdao Benzo Chemical Company (China). 2,2'-bis(1-hydroxyl-1-trifluoromethyl-2,2,2-triflutoethyl)-4,4'-methylenedianiline (BHTTM, $\geq$98.5%) was self-made in our lab. Piperazine (PIP, GR) was purchased from Sigma-Aldrich. The monomer structure is shown in Fig. 1. Sodium hydroxide (NaOH, AR), sodium hypochlorite (NaClO, CP) and n-hexane (AR) were obtained from Sinopharm Chemical Reagent Co. Ltd. (China).

2.2. Preparation of the composite NF membrane

The composite NF membranes were prepared with interfacial polymerization method. A series of aqueous phase solutions containing different ratios of PIP/BHTTM were prepared (the total diamine concentration was 1% w/v and the concentration of NaOH was 0.05 mol/L), whereas the organic phase solutions was composed of 0.15%w/v TMC in n-hexane. The PSF UF membrane was immersed into the deionized water for more than 5 h before using as porous support. Then the PSF UF membrane was taken out from the deionized water, air-drying until no visible droplet, and clamped with two PTFE frames which thickness was 0.6 cm and inner diameter was 12 cm. First, the aqueous solution was cast on the top surface of the PSF support membrane, kept in contact with the support membrane for 5 min before pouring the excess solution. An air knife was used to remove the residual droplet for 15 s. Second, the top surface of the membrane was covered with the organic solution for a few seconds to produce a thin PA layer on the substrate by interfacial polymerization. After removing the excess organic solution from the surface, the membrane was placed in ambient temperature for 1 min to let residual n-hexane evaporate completely. The newly formed membrane with the frame was heated in the oven at 80 °C for 5 min for further polymerization, and then stored in the deionized water for future use.

A series of certain concentration NaClO aqueous solutions were prepared. The composite NF membrane was immersed into the NaClO aqueous solution for different concentrations with some given time periods at room temperature. Finally, the oxidized NF was rinsed by the deionized water for 1 min, and stored in the deionized water until it was tested.

2.3. Characterization of the NF membrane

A series of standard characterization equipments were used to study the NF membranes physiochemical properties. To give more information and comparison with the membrane using PIP/BHTTM as the aqueous phase, two reference membranes were prepared by single component of PIP or BHTTM.

2.3.1. XPS analysis

The chemical compositions of top surfaces of the NF membranes were obtained by an X-ray photoelectron spectroscopy analysis (XPS; VG-miclab II, UK).

2.3.2. SEM analysis

The morphologies of the cross section and top surface of the NF membrane were observed by a scanning electron microscope (SEM, NOVA NANOSEM450) with the magnification times of 50,000.

2.3.3. AFM analysis

The topographic images and the roughness of top surface of the membrane were determined by AFM (Veeco, Nanoscope IIIa Multimode AFM), with 5 μm × 5 μm scanning range. The software Nanoscope was used to analyze the roughness of the membranes, Rms means the root mean square roughness, while Ra means the arithmetic mean roughness.

2.3.4. Dynamic water contact angle

The dynamic water contact angle (θ) of the NF membranes was

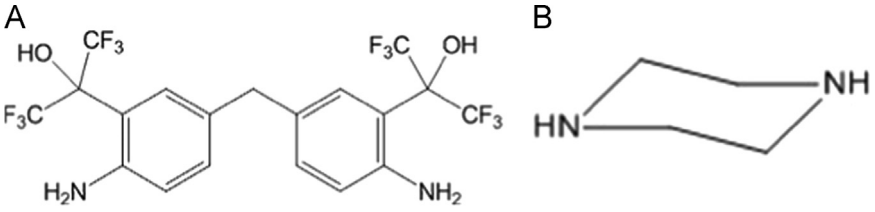

Fig. 1. The chemical structures of the monomers used in this study.A-BHTTM; B-PIP.

investigated by contact angle meter (JC2000A, Shanghai Zhong Cheng Digital Equipment Co., Ltd., China) at 25 °C. The total monitored time was 40 s and each point was collected in interval of 1 s. Each sample was measured 3 times and averaged.

2.4. Evaluation of the separation property of the NF membrane

Membrane performance was conducted with a label-scale cross-flow filtration stainless steel module, which had an effective area of $4.9 \times 4.9 \times \pi$ cm^2. The operating pressure was 0.6 MPa at room temperature about 20 °C. After compacting the NF membrane with DI water for 1 h, pure water flux was measured precisely. A series of salt solution (Na_2SO_4, $MgSO_4$ and NaCl, 2000 ppm) were used to characterize the NF membrane retention property and water permeation. Meanwhile the pore size and the MWCO of the membrane were measured by the neutral organic solution (gluceso, sucrose and raffinose, 300 ppm). The flux was calculated based on the formula as:

$$J = \frac{V}{A \times T} \tag{1}$$

Where J is the membrane flux (L/(m^2 h)), V is the volume of collected permeate liquid(L), A is the effective membrane area(m^2), T is the time to collect V permeate liquid(h).The rejection property was calculated by following formula:

$$R(\%) = (1 - \frac{C_p}{C_f}) \times 100 \tag{2}$$

Where C_f and C_p are the solute concentration in feed and permeate solutions, respectively.

For salt solution, the concentration was measured by DDS-11A

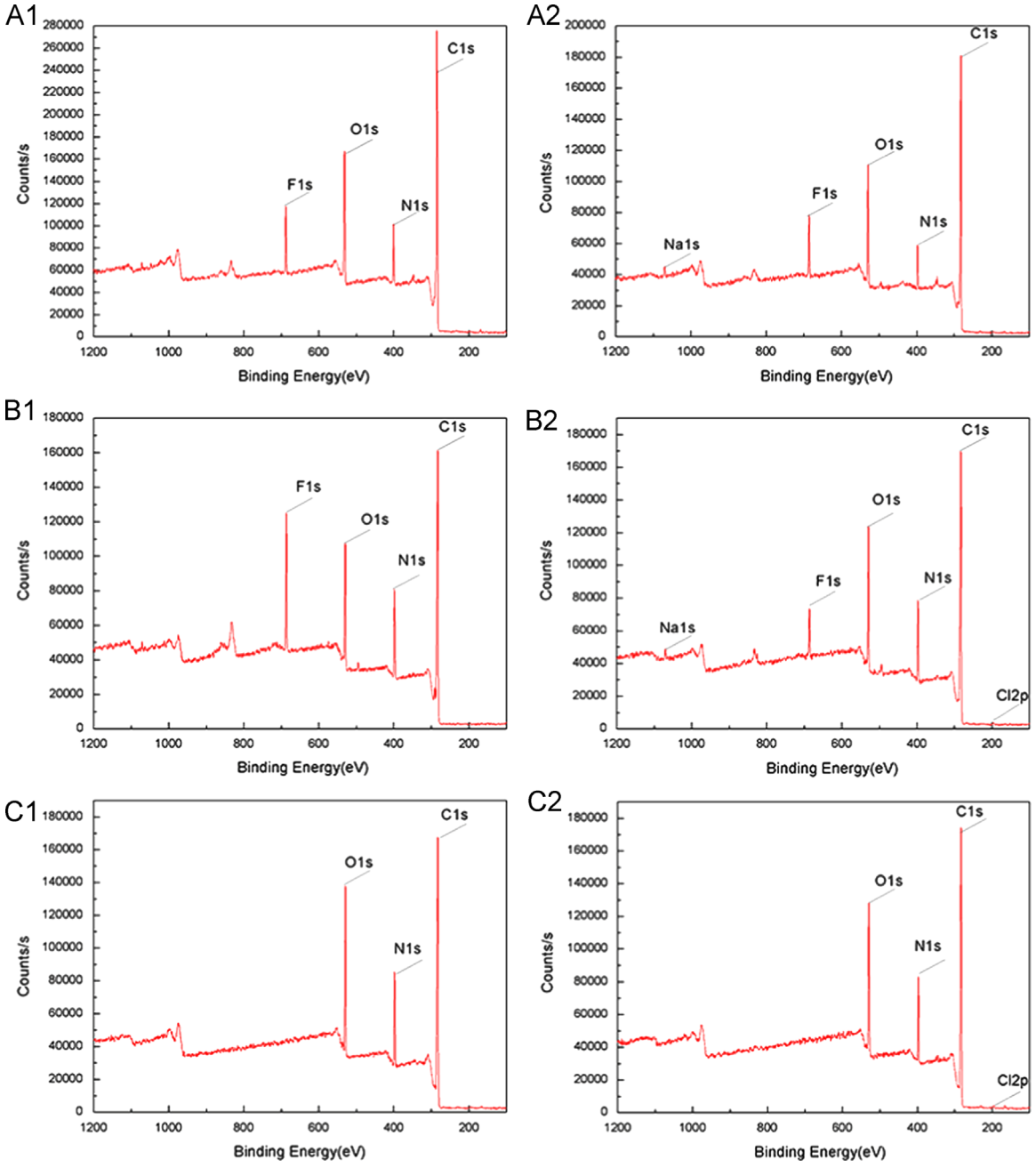

Fig. 2. XPS wide-scan spectra of the NF membranes.A1 – BHTTM only before oxidization; A2 – BHTTM only after oxidization; B1 – Mixed BHTTM/PIP before oxidization; B2 – Mixed BHTTM/PIP after oxidization; C1 – PIP only before oxidization; C2 – PIP only after oxidization.

Table 1
Elemental compositions of the NF membranes analyzed by XPS.

Sample	Atom percent (%)					
	C1s	N1s	O1s	F1s	Cl2p	Na1s
A1	70.93	8.74	15.11	5.22	0.00	0.00
A2	72.00	8.09	14.33	4.95	0.00	0.63
B1	66.76	11.42	12.01	9.82	0.00	0.00
B2	68.54	12.75	12.86	5.02	0.32	0.51
C1	70.18	14.04	15.78	0.00	0.00	0.00
C2	72.37	12.24	14.90	0.00	0.49	0.00

Note: A1-BHTTM only before oxidization; A2-BHTTM only after oxidization; B1-Mixed BHTTM/PIP before oxidization; B2-Mixed BHTTM/PIP after oxidization; C1-PIP only before oxidization; C2-PIP only after oxidization.

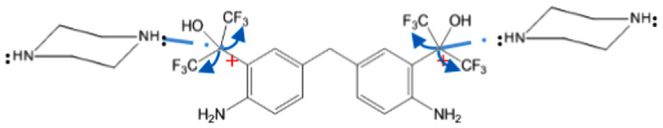

Fig. 3. The schematic diagram for the coordinate bond between BHTTM and PIP.

conductance meter (Shanghai Neici Instrument Company, China), and matched with the measured salt standard curve. For neutral organic solution, the concentration was measured by a TOC analyzer (Shimadzu, Model TOC_{VPN}, Japan).

3. Results and discussion

3.1. The chemical composition of top surface of the NF membrane

The surface chemical compositions of the NF membranes were analyzed by XPS shown in Fig. 2. The results are summarized in Table 1. From the spectra shown in Fig. 2, the NF membrane prepared from pure BHTTM has no evidence of chlorine after the post-oxidization. Whereas, the membrane prepared from PIP contains 0.49% chlorine after oxidization, which chlorine content is highest in all membranes. For the common polyamide membranes, the chlorination usually started with the amide N–Cl replace [22], so the content of Cl is the mainly factor to evaluate the chlorination. For the PIP, the lack of amide protons accounts for the low chlorine incorporation into PIP membranes. But the chlorination still occur at the low abundance noncross-linked nitrogen atoms [23,24]. And for the BHTTM, even in rich of amide protons, but for the existence of $–CF_3$, no Cl can be detected. So the BHTTM has more chlorine resistance ability. Compared with the pure PIP membrane, the NF membrane incorporating BHTTM/PIP after oxidization has much lower level of chlorine about 0.32%. In particular, its fluorine content is 5.02%, which is basically the same as the NF membrane prepared by the pure BHTTM after oxidization. These demonstrate the NF membrane prepared by mixed BHTTM/PIP has a certain ability for chlorine resistance.

For A2 and B2 has a little content of Na, this is mainly due to the existence of fluorine, Wang et al. [25] cleaned the PVDF membrane with NaOH or NaClO, and the XPS result shows the membrane will have the Na after the chemical clean. An interesting phenomenon is sample B1 has the highest content of F and after the post-oxidation treatment, the F content decreased significantly. A hypothetical explanation was arise to figure out the abnormal phenomenon. For the hydrophobicity of $–CF_3$, the reactivity of $–NH_2$ and the steric hindrance, the exposure of F for the BHTTM was low. But as Fig. 3 shows, PIP and BHTTM would form the coordinate bond, and for the low molecular mass of PIP, PIP can permeate though the membrane easily, so more F would exposure on the membrane surface. While on the BHTTM/PIP membrane top surface, the content of PIP was high, and the PIP will degrade in the oxidation treatment. As the SEM shown, the thickness of BHTTM/PIP and top surface will change after the post-oxidation, the degradation of PIP will also cause the decrease of F on the membrane surface.

3.2. NF membrane morphologies

SEM and AFM were used to characterize the structure and surface roughness of the NF membranes. Fig. 4 shows the SEM images of the surface morphology and the cross-section of the PSF support membrane. And Fig. 5 represents the morphologies of the NF membrane made by pure BHTTM, mixed BHTTM/PIP (50% BHTTM+50%PIP) and pure PIP, respectively. The left is the membrane prepared before oxidation while the right is the membranes prepared after oxidation by the NaClO aqueous solution (3000 ppm, 1 h). In Fig. 5 A1, the NF membrane prepared from BHTTM has a polyamide layer of 100 nm with smoothest surface before oxidation. A2 reveals that the thickness of NF membrane is reduced to 91 nm, and the surface becomes rougher after oxidation. While the increased surface roughness and decreased membrane thickness can finally enhance the permeate flux [26]. In B1, NF membrane prepared from the mixed BHTTM/PIP has a thickness of 440 nm, and the membrane surface is rougher than in A1. After oxidation, the thickness of the membrane is reduced to

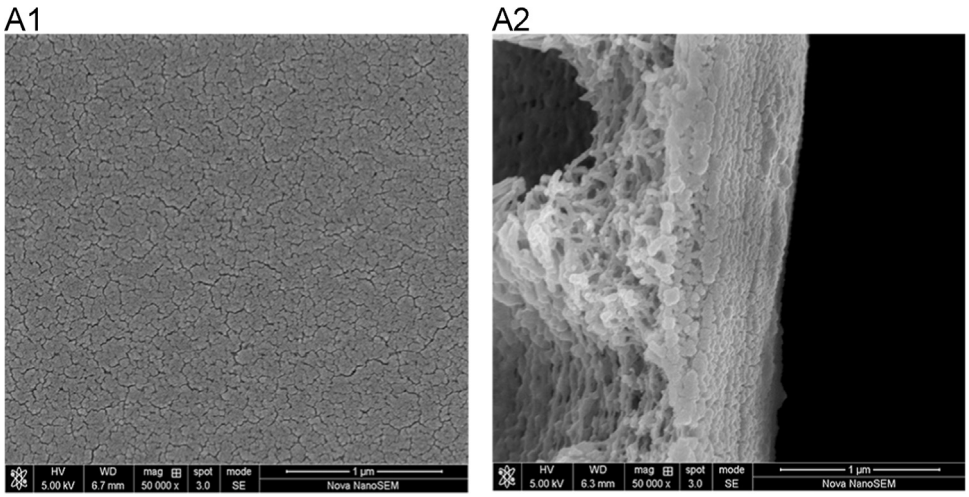

Fig. 4. The morphology of the PSF supporting membrane. A1 – Top surface; A2 – Cross-section.

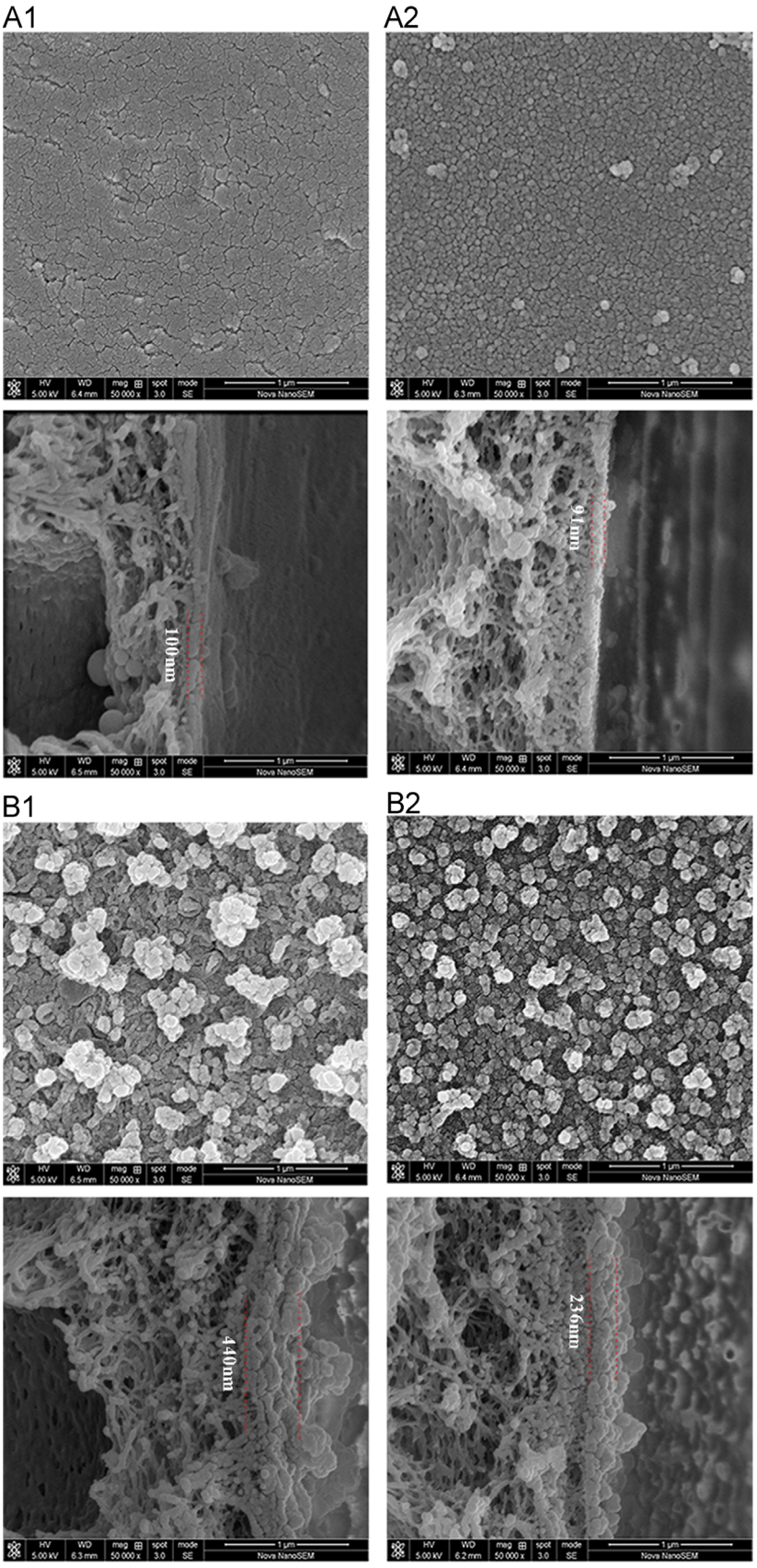

Fig. 5. SEM images of the cross-section and surface of NF membranes.A1 – BHTTM before oxidization; A2 – BHTTM after oxidization; B1 – BHTTM/PIP before oxidization; B2 – BHTTM/PIP after oxidization; C1 – PIP before oxidization; C2 – PIP after oxidization.

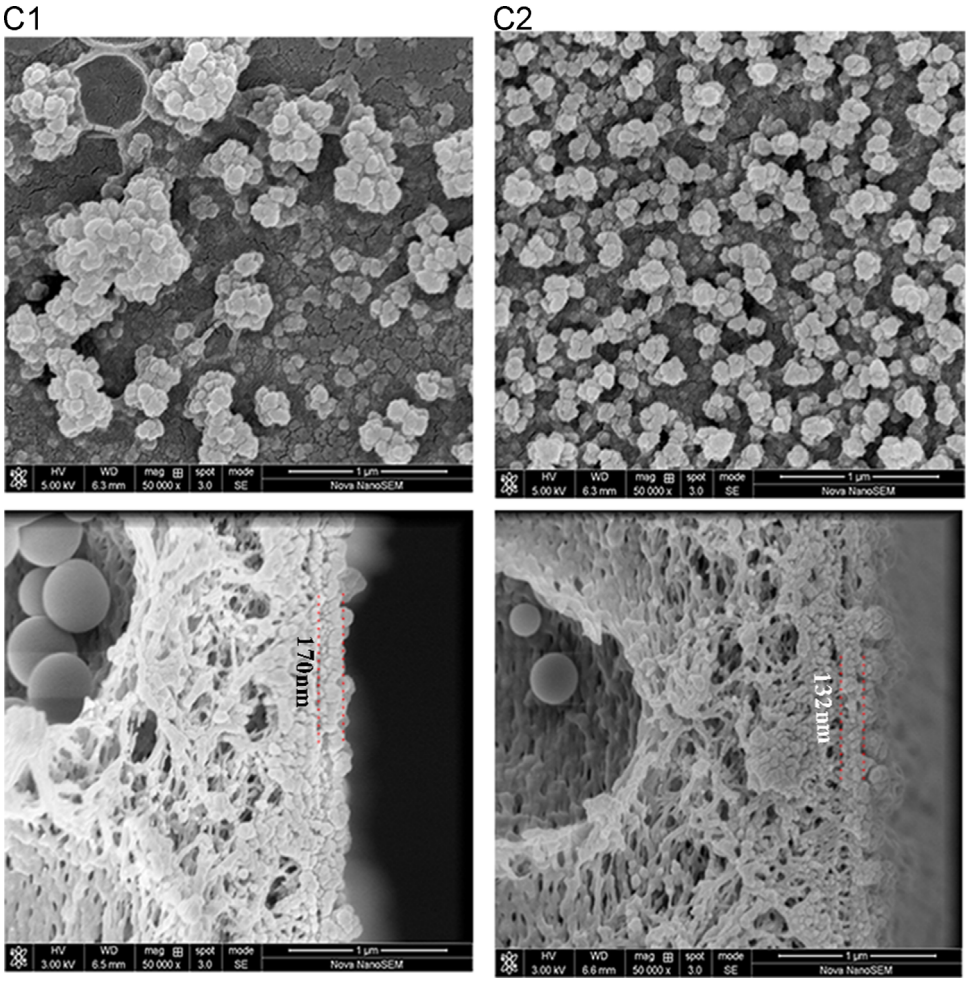

Fig. 5. (*continued*)

236 nm, and those bumps on membrane surface become smaller, shown in B2. In C1, the NF membrane fabricated from PIP has the thickness of 170 nm. After oxidation, the thickness of NF membrane significantly decreases from 170 nm to 132 nm, and some obvious defect can be seen in C2. This means that the membrane prepared from PIP has a very low tolerance to active chlorine. For the electron-withdrawing fluorine–containing group of BHTTM, the membranes with single BHTTM and mixed BHTTM/PIP after being treated by the NaClO (3000 ppm, 1 h) still maintain complete structures without any obvious defect. The AFM result is illustrated in Fig. 6. A is the PSF membrane, which surface is as smooth as the appearance in SEM picture. B1 is the membrane prepared by pure BHTTM (before oxidation), which is smooth and with some small prominent bumps, while the prominent bumps in B2 atrophy a little after oxidation. C1 and C2 are the membranes incorporated with BHTTM and PIP before oxidation and after oxidation, the roughness and the prominent bumps experience slightly change. The NF membrane using PIP alone undergo observably change during oxidization, which is demonstrated in D1 and D2. And the roughness Ra and Rms is shown in Table 2.

For the poly(piperazine-amide) cannot tolerant the free chlorine, and it will degrade in the existence of NaClO. The same conclusion can be seen in the following Ref. [24,27]. The Figs. 5 C-1,C-2 and 6D-1,D-2 show the poly(piperazine-amide) NF membranes surface changed a lot after NaClO post treatment, and the polyamide layer become thin and obvious defect can be seen. For the BHTTM/PIP NF membrane, during the IP process, PIP can easy permeate though the interface for its low molecule weight, so the top surface of the BHTTM/PIP NF membrane is mainly PIP. For the lack chlorine tolerance of PIP, the top polyamide layer of BHTTM/PIP NF membrane will degrade during the post-oxidation process, so the thickness was declined and the membrane surface specific surface area was enlarged. For the BHTTM NF membrane, the thickness of the polyamide was not changed a lot, but the membrane surface specific surface area was enlarged.

3.3. The hydrophilicity of the NF membrane

The dynamic contact angles are measured to evaluate the hydrophilicity of the NF membrane in Fig. 7. NF membrane prepared from pure PIP has the smallest dynamic contact angle of 16.5° compared with the dynamic contact angles (around 25°) of the membranes prepared from BHTTM or BHTTM/PIP mixture. Moreover, the oxidation process by NaClO (3000 ppm, 1 h) has a significant influence on the dynamic contact angles of the membranes. All membranes showed that the dynamic contact angles are increased after the oxidation process, from 16.5° to 20° for PIP membrane, from 25° to 30° for BHTTM/PIP membrane and from 58° to 67° for BHTTM membrane, respectively. An increase of BHTTM ratio leads to a higher dynamic contact angle due to the hydrophobic property of BHTTM [17].

3.4. Effect of reaction time on the NF membrane performance

The reaction time is an important factor affecting the interfacial polymerization reaction process. The reaction time of interfacial

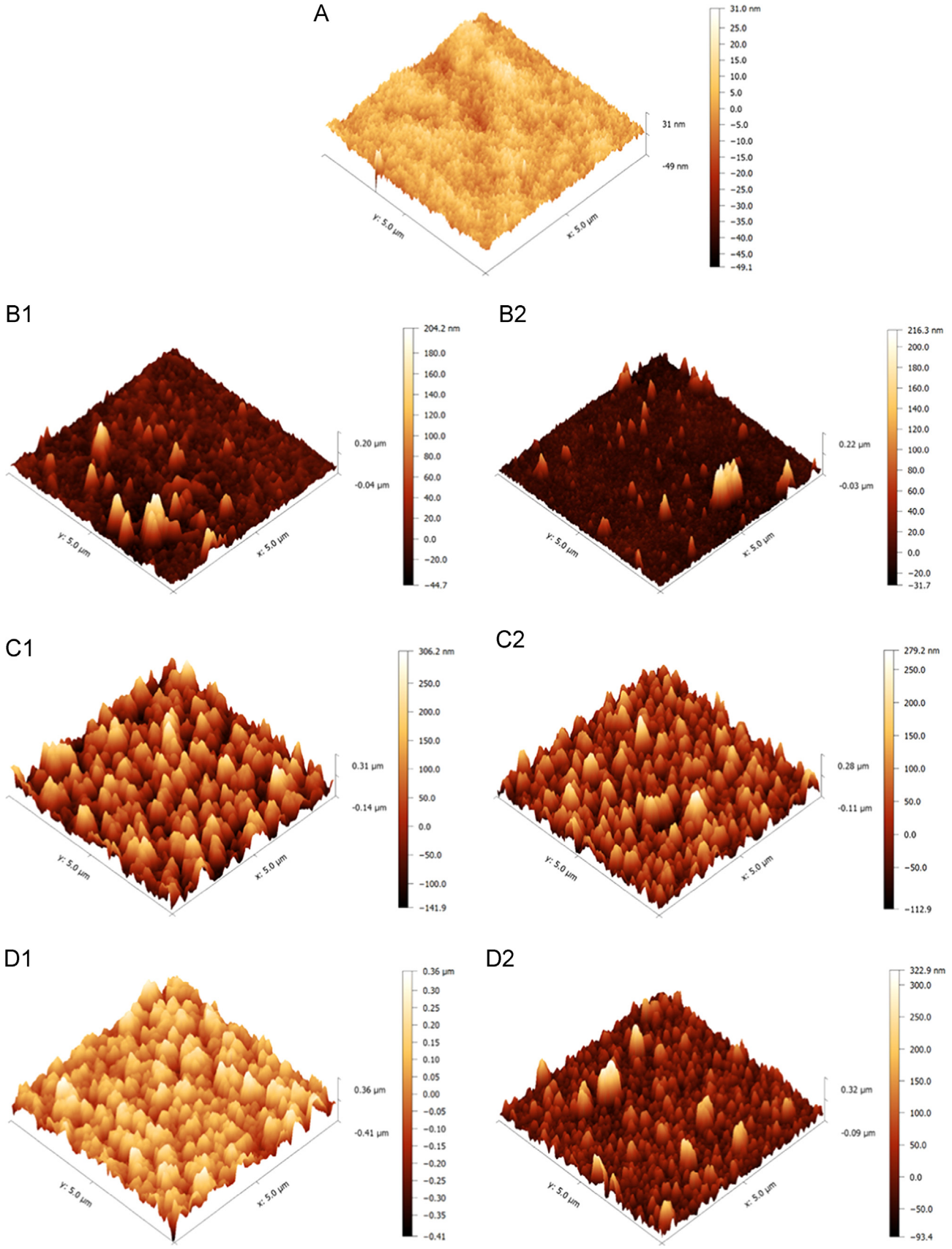

Fig. 6. AFM images of NF membranes.A – PSF membrane supporter; B1 – BHTTM before oxidization; B2 – BHTTM after oxidization; C1 – BHTTM/PIP before oxidization; C2 – BHTTM/PIP after oxidization; D1 – PIP before oxidization; D2 – PIP after oxidization.

Table 2
The roughness of the NF membrane.

Membranes	Ra (nm)	Rms (nm)
Support membrane	4.39	5.57
BHTTM(before oxidization)	14.6	23.8
BHTTM(after oxidization)	9.84	19.1
BHTTM-PIP(before oxidization)	66.0	79.2
BHTTM-PIP(after oxidization)	46.7	57.5
PIP(before oxidization)	85.6	104
PIP(after oxidization)	34.3	47.8

polymerization from 5 s to 30 s was investigated. The effect of reaction time on the NF membrane performance is shown in Fig. 8. It can be seen that with the reaction time increases, the pure water flux decreases, 53.9 L/(m^2 h) for 5 s and 52.1 L/(m^2 h) for 15 s, respectively. The salt rejection increased from 97.9% to 99.5%. The reason should be related to the change of the thickness of polyamide layer. After the reaction time prolongs from 15 s to 30 s, no obviously change is observed. This means the reaction time of 15 s is the optimized reaction time.

3.5. *Effect of BHTTM/PIP ratio on the NF membrane performance*

Effect of BHTTM/PIP ratio on NF membrane performance is shown in Fig. 9. It can be seen that the NF membrane prepared from pure BHTTM possesses the water flux 8.14 L/ (m^2 h) and the salt rejection 95.7%. It has much difference with the NF membrane fabricated by BHTTM alone on the PES UF membrane in our previous work [19]. The NF membrane prepared on the PES UF membrane had a higher flux with 10.1 L/ (m^2 h) and a lower salt rejection with 85.3%, this is mainly ascribed to the nature of the different support membranes. The NF membrane made of PSF UF membrane has a higher crosslinking degree and the polyamide layer becomes more compact [28]. As the proportion of PIP increased from 0% to 20%, it leads to the improvement in water flux and the decrease in salt rejection. The decline of the rejection is due to the competing effect between the two monomers [20,29,30]. According to the discussion in Section 3.2, the improvement of the flux could be explained as the increased surface roughness with the addition of PIP into the aqueous phase solution.

When PIP content increases from 20% to 50%, both the salt rejection and flux increase. It could be explained that the addition of PIP might improve the cross-linking density and the roughness just as the SEM result is shown in Fig. 3.

Nevertheless, a further increased ratio of PIP from 50% to 100% causes a decreased flux of NF membrane. This could be attributed to the reduced effective membrane surface. As the SEM result shows, the PIP-BHTTM membrane surface is more uniform, while the pure PIP membrane surface suffered serious conglomeration,

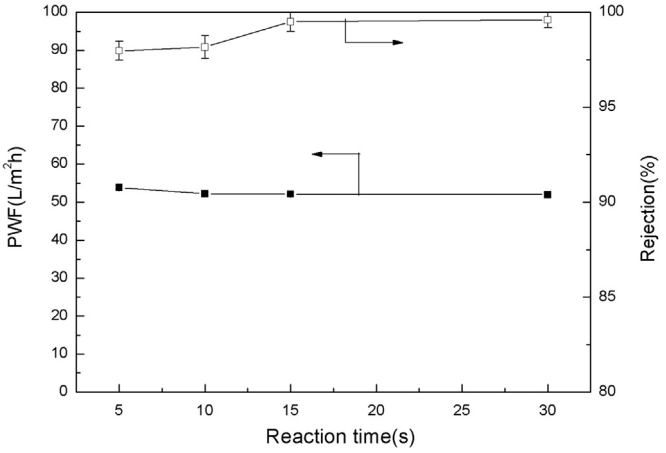

Fig. 8. The effect of reaction time on the NF membranes performance.

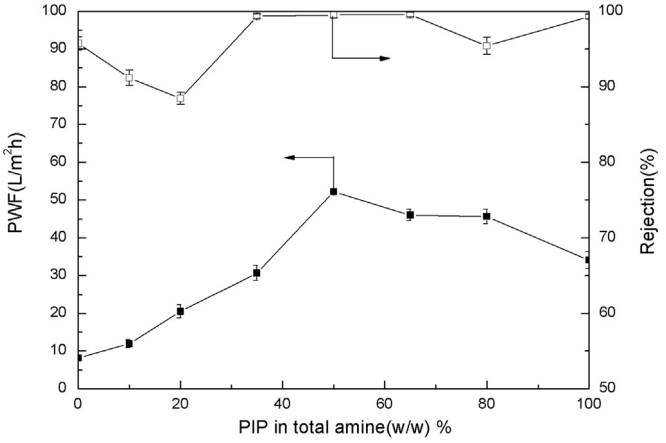

Fig. 9. The effect of BHTTM/PIP mixing ratio on the composite NF membranes performance before oxidation.

leading the effective membrane surface reduced.

The above is the effect of BHTTM/PIP mixing ratio on composite membrane performance before oxidation. Fig. 10. illustrates how the mixing ratio of diamine monomer influences the performance of membrane after oxidation by NaClO (3000 ppm, 1 h). The fluxes of the membranes after oxidation all are improved greatly, and the salt rejection has still kept on a high level (the pure PIP cannot tolerant the active chloride, so it is not shown in the figure). The phenomenon is probably that the membrane layer becomes thinner and the surface prominent bumps become more uniform after oxidation, which is consistent with the SEM pictures. In other words, the mass transfer resistance becomes smaller and the effective membrane area increases. Hence, the PIP ratio of 50% is the

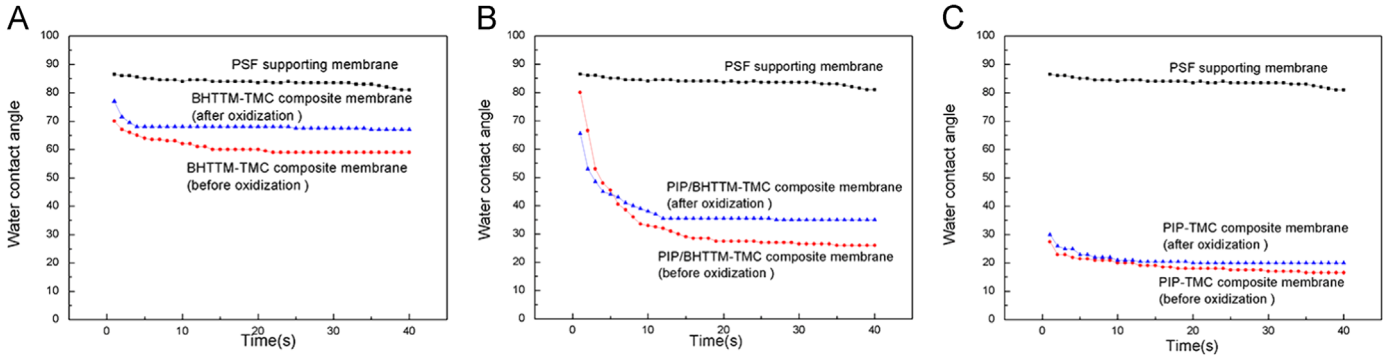

Fig. 7. The dynamic contact angles of PSF membrane support and prepared NF membranes.

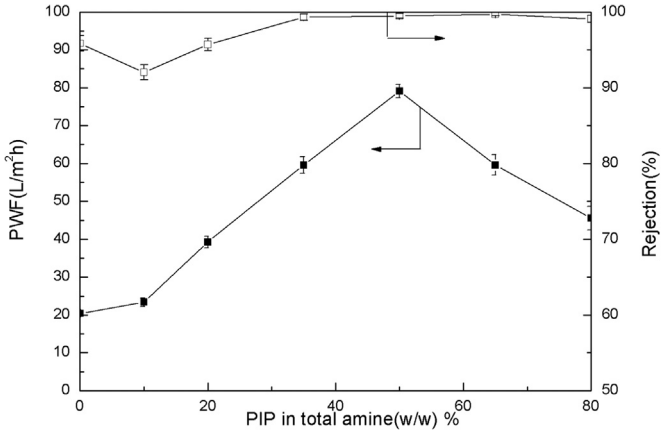

Fig. 10. The effect of BHTTM/PIP mixing ratio on the composite NF membranes performance after oxidation. (Oxidation condition: 3000 ppm NaClO, 1 h).

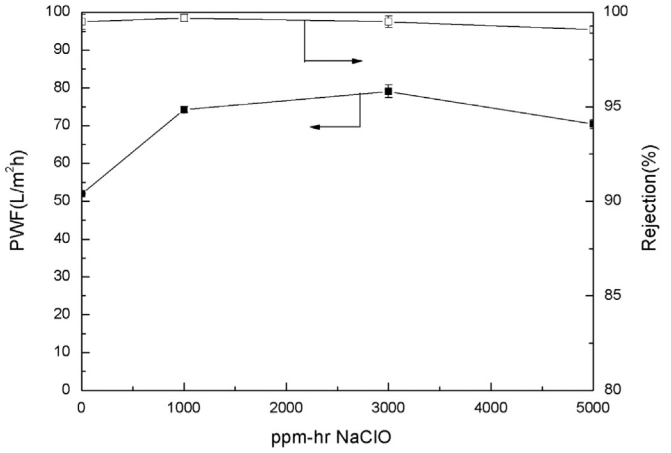

Fig. 11. The effect of oxidation treatment by different concentration of chlorine solutions on Na_2SO_4 rejection and water flux of NF membrane.

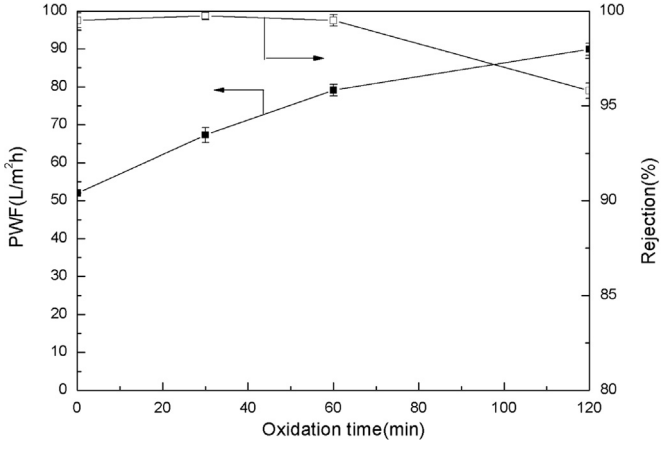

Fig. 12. The effect of oxidation treatment by different oxidation times of chlorine solution on Na_2SO_4 rejection and water flux of NF membrane.

Table 3
The rejections of different neutral solutes of the NF membrane (BHTTM-PIP after oxidization by 3000 ppm NaClO 1 h).

Solute	Molecular weight (Da)	Stokes radius (nm)	Solute rejection (%)
Glucose	180	0.359	71.6 ± 1.5
Sucrose	342	0.462	94.9 ± 1.7
Raffinose	504	0.538	96.9 ± 1.0

Table 4
The rejections of different salts and permeate flux of the NF membrane (BHTTM-PIP after oxidization by 3000 ppm NaClO 1 h).

Salt	Rejection (%)	Permeate flux (L/m² h)
Na_2SO_4	99.5 ± 0.4	72.0 ± 2.8
$MgSO_4$	95.0 ± 1.3	65.8 ± 2.0
NaCl	30.0 ± 1.2	72.4 ± 1.7

optimized mixing ratio.

3.6. Effect of the oxidization condition on the NF membrane performance

Different NaClO concentration (1000 ppm, 3000 ppm, 5000 ppm; 60 min) and oxidization time (3000 ppm; 30 min, 60 min, 120 min) are used to investigate their effect on the NF membrane in Figs. 11 and 12. When the concentration of chlorine solution is 1000 ppm, the water flux is increased from 52.1(L/m² h) to 74.3(L/m² h), and the salt rejection is improved from 99.5% to 99.7%. After the concentration of chlorine solution reaches 3000 ppm, the salt rejection is not the obvious change from 99.7% to 99.5%. But the water flux is increased from 74.3(L/m² h) to 79.1 (L/m² h). The flux change could be related to the membrane thickness and surface roughness. The salt rejection change could be explained by tightening up effect [19,31]. At low NaClO concentration, the oxidation effect could increase the crosslink degree of the polyamide chains.

When the oxidation time is 0.5 h, the flux increases from 52.1 (L/m² h) to 67.3 (L/m² h) and the salt rejection is improved from 99.5% to 99.7%; And when the oxidation time continues to 1 hour, the salt rejection declines a bit from 99.7% to 99.5%, and the water flux is improved from 67.3 (L/m² h) to 79.1 (L/m² h). A little difference between the two figures is the last point. This could be explained that oxidation time has a greater impact than NaClO concentration on NF membrane. Over long oxidation time is likely to cause irreversible damage to the NF membrane. Therefore, the optimized oxidation condition is 3000 ppm-h.

3.7. The separation property of the NF membrane

In this section, the BHTTM-PIP NF membrane prepared with the optimized conditions was investigated to evaluate its potential application. The optimum condition is as follows: 0.5% (w/v) BHTTM+0.5% (w/v) PIP in the aqueous phase; 0.15%TMC in the organic phase; reaction time for 15 s; curing temperature at 80 °C for 5 min, and finally oxidized by 3000 ppm NaClO solution for 1 h. The testing condition was using 300 ppm neutral organic solution (Gluceso, sucrose and raffinose) to confirm the NF pore size and the MWCO, and using 2000 ppm salt solution (Na_2SO_4, $MgSO_4$ and NaCl) to characterize the NF membrane retention property and water permeation.

Table 3 shows the rejection of the NF membrane for various neutral solutes. Obviously, the MWCO of the NF membrane is under 300 Da, and the corresponding effective pore size is about 1 nm, which is a typical NF characteristic number. The rejections of different salt solutions and the permeate fluxes are shown in Table 4. It can be seen that the salt rejection of the NF membrane decreased in the following order: $Na_2SO_4 > MgSO_4 > NaCl$, which indicates the NF membrane is a negatively charged membrane. In addition, the rejections of divalent anions are much higher than mono-valent anions.

The NF membrane developed in the current work are compared with several commercially available NF membranes in Table 5. The performance of the BHTTM/PIP (after oxidization) NF membranes

Table 5
Comparison of the current NF membranes to various commercially available NF membranes.

Membrane	PWF (l/m^2 h bar)	MWCO(Da)	Stabilized salt rejection (%)			Salt concentration (ppm)	Operating pressure (bar)	References
			Na_2SO_4	$MgSO_4$	NaCl			
BHTTM/PIP(Before oxidation)	8.7	–	99.5	–	–	2000	6	Current work
BHTTM/PIP(After oxidation)	13.2	< 300	99.5	95	30	2000	6	
Synder NFW	5.4	300–500	–	97	20	2000	8.3	[3,32]
Synder NFX	2.4	150–300	–	99	40	2000	8.3	[3]
GE-Osmonics HL	6.9	150–300	–	97	33	1000	7.6	[20,3]
GE-Osmonics DL	10	150–300	–	96	< 40	5000	30	[3,33]
DOW-Filmtec NF90	6.7	200–400	–	98	90	2000	4.8	[20,3]
DOW-Filmtec NF70	7.2	200–400	–	97	70	2000	4.8	[34]

Table 6
The chlorine tolerance of the commercial NF membranes.

Brand	Products	Chlorine tolerance	References
DOW	FILMTEC^{TM} NF245-3838	Non-detectable	[35]
	FILMTEC^{TM} NF245-3840	Non-detectable	[35]
	FILMTEC^{TM} NF270-400/34i	< 0.1 ppm	[35]
	FILMTEC^{TM} NF90-400/34i	< 0.1 ppm	[35]
GE	DK Series	500 ppm h	[36]
	DL Series	500 ppm h	[36]
Toray	SU610	Non-detectable	[37]
	SU620	Non-detectable	[37]
	SU620F	Non-detectable	[37]
Hydranautics	DairyNFTM	Non-detectable	[38]
	ESNA1-4040	Non-detectable	[38]
	ESNA1-K1	Non-detectable	[38]
	ESNA1-LF2	Non-detectable	[38]

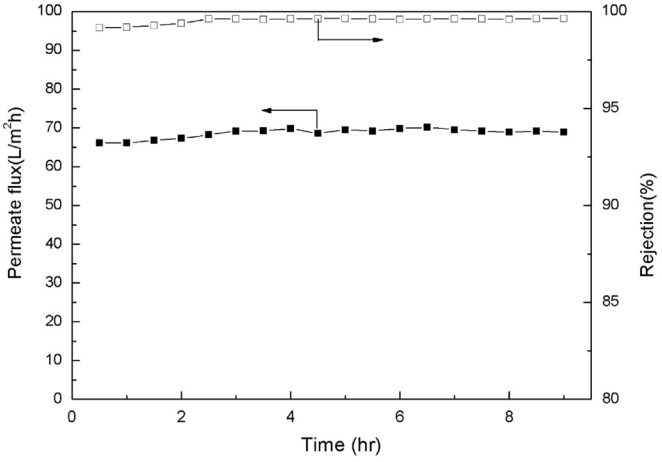

Fig. 13. Long-term testing of the NF membrane during 10 h (0.6 MPa, 2000 ppm Na_2SO_4).

appears to be superior to all the commercial membranes. Furthermore, the chlorine tolerance of the commercial NF membranes (seen in Table 6) is much lower than the NF membrane developed in this work (3000 ppm h).

3.8. The stability of the NF membrane in long-time running

The performance stability is very important for the NF membrane practical application. The long-time running test is under the following condition: the operating pressure is 0.6 MPa, the Na_2SO_4 concentration is 2000 ppm and the operating temperature is 20 ± 0.5 °C. Fig. 13 shows that the long-time running for the NF membrane is very well in 10 h. Both the rejection and the flux are a little increasing in the initiative two hours. Then, the rejection remains the stable value with 99.5%. And the water flux is varied from 65 (L/m^2 h) to 70 (L/m^2 h). Therefore, the NF membrane shows robust performance in the long-time running.

4. Conclusion

NF membrane with good chlorine resistance and desalination performance was prepared by using the mixed diamine of PIP/BHTTM in interfacial polymerization process. The effects of interfacial polymerization reaction time, BHTTM/PIP mixing ratio, and oxidation condition on the NF membrane performance were studied thoroughly. The optimized NF membrane was prepared by the following conditions: 0.5% (w/v) BHTTM + 0.5% (w/v) PIP in the aqueous phase; 0.15% (w/v) TMC in the organic phase; the reaction time was 15 s; the curing temperature was 80 °C for 5 min; and finally oxidized by 3000 ppm NaClO solution for 1 h. The MWCO of the optimized NF membrane was below 300 Da, the corresponding effective pore size was about 1 nm, and the pure water flux was 79.1 (L/m^2 h). The rejections of the optimized NF membrane for Na_2SO_4, $MgSO_4$ and NaCl were 99.5%, 95% and 30%, respectively. The order of different salt rejections indicated the NF membrane was a typical negatively charged membrane.

Acknowledgment

The authors are thankful for the financial support received from 2013 Special Project of the Development and Industrialization of New Materials of National Development and Reform Commission in China (20132548), the National Science and Technology Support Project of China (2014BAB07B01), the Key Technology R&D Program of Shanghai Committee of Science and Technology in China (13521102000) and the Key Technology R&D Program of Jiangsu Committee of Science and Technology in China (BE2013031).

References

[1] X. Fan, Y. Dong, Y. Su, X. Zhao, Y. Li, J. Liu, Z. Jiang, Improved performance of composite nanofiltration membranes by adding calcium chloride in aqueous phase during interfacial polymerization process, J. Membr. Sci. 452 (2014) 90–96.
[2] D. Hu, Z.-L. Xu, Y.-M. Wei, Y.-F. Liu, Poly(styrene sulfonic acid) sodium modified nanofiltration membranes with improved permeability for the softening of highly concentrated seawater, Desalination 336 (2014) 179–186.
[3] A.W. Mohammad, Y.H. Teow, W.L. Ang, Y.T. Chung, D.L. Oatley-Radcliffe, N. Hilal, Nanofiltration membranes review: Recent advances and future prospects, Desalination 356 (2015) 226–254.
[4] D. Hu, Z.-L. Xu, C. Chen, Polypiperazine-amide nanofiltration membrane containing silica nanoparticles prepared by interfacial polymerization, Desalination 301 (2012) 75–81.

[5] J.-Q. Liu, Z.-L. Xu, X.-H. Li, Y. Zhang, Y. Zhou, Z.-X. Wang, X.-J. Wang, An improved process to prepare high separation performance PA/PVDF hollow fiber composite nanofiltration membranes, Sep. Purif. Technol. 58 (2007) 53–60.
[6] M. Homayoonfal, A. Akbari, M.R. Mehrnia, Preparation of polysulfone nanofiltration membranes by UV-assisted grafting polymerization for water softening, Desalination 263 (2010) 217–225.
[7] B.A.M. Al-Rashdi, D.J. Johnson, N. Hilal, Removal of heavy metal ions by nanofiltration, Desalination 315 (2013) 2–17.
[8] A. Maher, M. Sadeghi, A. Moheb, Heavy metal elimination from drinking water using nanofiltration membrane technology and process optimization using response surface methodology, Desalination 352 (2014) 166–173.
[9] X. Wei, X. Kong, S. Wang, H. Xiang, J. Wang, J. Chen, Removal of heavy metals from electroplating wastewater by thin-film composite nanofiltration hollow-fiber membranes, Ind. Eng. Chem. Res 52 (2013) 17583–17590.
[10] A.N. Negrão Murakami, R.D. de Mello Castanho Amboni, E.S. Prudêncio, E. R. Amante, L. de Moraes Zanotta, M. Maraschin, J.C. Cunha Petrus, R.F. Teófilo, Concentration of phenolic compounds in aqueous mate (*Ilex paraguariensis* A. St. Hil) extract through nanofiltration, Food Sci. Technol. 44 (2011) 2211–2216.
[11] H.B. Park, B.D. Freeman, Z.-B. Zhang, M. Sankir, J.E. McGrath, Highly chlorine-tolerant polymers for desalination, Angew. Chem. Int. Ed. 47 (2008) 6019–6024.
[12] L. Ni, J. Meng, X. Li, Y. Zhang, Surface coating on the polyamide TFC RO membrane for chlorine resistance and antifouling performance improvement, J. Membr. Sci. 451 (2014) 205–215.
[13] J. Xu, Z. Wang, L. Yu, J. Wang, S. Wang, A novel reverse osmosis membrane with regenerable anti-biofouling and chlorine resistant properties, J. Membr. Sci. 435 (2013) 80–91.
[14] Y. Gao, A.M.S. de Jubera, B.J. Mariñas, J.S. Moore, Nanofiltration membranes with modified active layer using aromatic polyamide dendrimers, Adv. Funct. Mater. 23 (2013) 598–607.
[15] H. Zhao, S. Qiu, L. Wu, L. Zhang, H. Chen, C. Gao, Improving the performance of polyamide reverse osmosis membrane by incorporation of modified multi-walled carbon nanotubes, J.Membr.Sci 450 (2014) 249–256.
[16] W. Choi, J. Choi, J. Bang, J.-H. Lee, Layer-by-layer assembly of graphene oxide nanosheets on polyamide membranes for durable reverse-osmosis applications, ACS Appl. Mater. Interfaces 5 (2013) 12510–12519.
[17] Y.-H. La, J. Diep, R. Al-Rasheed, M. Nassar, E. Idil Mouhoumed, A. Szymczyk, G. Dubois, The effect of cross-contamination in the sequential interfacial polymerization on the RO performance of polyamide bilayer membranes, J. Membr. Sci 466 (2014) 348–356.
[18] The United States Pantent: US 20140042082A.
[19] D. Hu, Z.-L. Xu, Y.-M. Wei, A high performance silica–fluoropolyamide nanofiltration membrane prepared by interfacial polymerization, Sep. Purif. Technol. 110 (2013) 31–38.
[20] W. Fang, L. Shi, R. Wang, Mixed polyamide-based composite nanofiltration hollow fiber membranes with improved low-pressure water softening capability, J. Membr. Sci. 468 (2014) 52–61.
[21] L. Shao, X.Q. Cheng, Y. Liu, S. Quan, J. Ma, S.Z. Zhao, K.Y. Wang, Newly developed nanofiltration (NF) composite membranes by interfacial polymerization for Safranin O and Aniline blue removal, J. Membr. Sci. 430 (2013) 96–105.
[22] S. Avlonitis, W.T. Hanbury, T. Hodgkiess, Chlorine degradation of aromatic polyamides, Desalination 85 (1992) 321–334.
[23] V.T. Do, C.Y. Tang, M. Reinhard, J.O. Leckie, Effects of chlorine exposure conditions on physiochemical properties and performance of a polyamide membrane–mechanisms and implications, Environ. Sci. Technol. 46 (2012) 13184–13192.
[24] V.T. Do, C.Y. Tang, M. Reinhard, J.O. Leckie, Degradation of polyamide nanofiltration and reverse osmosis membranes by hypochlorite, Environ. Sci. Technol. 46 (2012) 852–859.
[25] L. Wang, Q. Wang, Y. Li, H. Lin, Ultrasound-assisted chemical cleaning of polyvinylidene fluoride membrane fouled by lactic acid fermentation broth, Desalination 326 (2013) 103–108.
[26] M. Hirose, H. Ito, Y. Kamiyama, Effect of skin layer surface structures on the flux behaviour of RO membranes, J. Membr. Sci. 121 (1996) 209–215.
[27] A. Simon, L.D. Nghiem, P. Le-Clech, S.J. Khan, J.E. Drewes, Effects of membrane degradation on the removal of pharmaceutically active compounds (PhACs) by NF/RO filtration processes, J. Membr. Sci. 340 (2009) 16–25.
[28] N. Misdan, W.J. Lau, A.F. Ismail, T. Matsuura, D. Rana, Study on the thin film composite poly(piperazine-amide) nanofiltration membrane: Impacts of physicochemical properties of substrate on interfacial polymerization formation, Desalination 344 (2014) 198–205.
[29] A.L. Ahmad, B.S. Ooi, A.W. Mohammad, J.P. Choudhury, Composite nanofiltration polyamide membrane: a study on the diamine ratio and its performance evaluation, Ind. Eng. Chem. Res. 43 (2004) 8074–8082.
[30] N.K. Saha, S.V. Joshi, Performance evaluation of thin film composite polyamide nanofiltration membrane with variation in monomer type, J. Membr. Sci. 342 (2009) 60–69.
[31] G.-D. Kang, C.-J. Gao, W.-D. Chen, X.-M. Jie, Y.-M. Cao, Q. Yuan, Study on hypochlorite degradation of aromatic polyamide reverse osmosis membrane, J. Membr. Sci. 300 (2007) 165–171.
[32] F. Zhao, K. Xu, H. Ren, L. Ding, J. Geng, Y. Zhang, Combined effects of organic matter and calcium on biofouling of nanofiltration membranes, J. Membr. Sci. 486 (2015) 177–188.
[33] A.R. Guastalli, J. Labanda, J. Llorens, Separation of phosphoric acid from an industrial rinsing water by means of nanofiltration, Desalination 243 (2009) 218–228.
[34] L. Meihong, Y. Sanchuan, Z. Yong, G. Congjie, Study on the thin-film composite nanofiltration membrane for the removal of sulfate from concentrated salt aqueous: preparation and performance, J. Membr. Sci. 310 (2008) 289–295.
[35] ⟨http://www.dow.com/en-us/water-and-process-solutions/products/reverse-osmosis⟩.
[36] ⟨https://www.gewater.com/kcpguest/⟩.
[37] ⟨http://www.toraywater.com/⟩.
[38] ⟨http://www.hydranautics.cn/products/nanofiltration/22.html⟩.